Fluorescence Spectroscopic Analysis of Silver Nanoparticles Interaction with Bovine Serum Albumin and Its Biological Implications

Supriya Chougale[1], Suraj Kumbhar[2], Rupali Chavan[3], Sneha Koparde[4], Prashant Sanadi[5], Nisha Nerlekar[6], Padma Dandge[7], Govind Kolekar[8], Ashok Chougale[9], Vishal Kumar More[10]
[1,2,3,9,10]*Department of Chemistry, The New College Kolhapur, Shivaji University, Kolhapur, (MS) India, 416003*
[4]*Department of Chemistry, Shivaji University, Kolhapur, (MS) India 416004*
[5,8]*Department of Engineering Chemistry, Kolhapur Institute of Technology's College of Engineering (Autonomous), Kolhapur Affiliated Shivaji University Kolhapur, 416004-India*
[6,7]*Department of Biochemistry, Shivaji University, Kolhapur, (MS) India 416004*

Abstract*—Nanoparticles (NPs) come into contact with protein-containing fluids, such as biological fluids, and they quickly accumulate a layer of proteins on their surface, known as the protein corona. The composition and structure of this protein corona are crucial for determining how the nanoparticles interact with living cells. The interaction between silver nanoparticles (AgNPs) and bovine serum albumin (BSA) was examined using various methods, including fluorescence quenching, dynamic light scattering (DLS), and zeta potential analysis. The adsorption resulted in a significant gradual increase in the average hydrodynamic radius of the AgNPs protein corona from 30nm to 40nm. Changes in the zeta potential charge on the surface of AgNPs, and the AgNPs protein corona led to an increase in stability in the AgNPs protein corona compared to AgNPs (-18 to -30 (mV). Functional groups of AgNPs were changed by protein functional groups, as revealed by FT-IR analysis. Scanning Electron Microscopy (SEM) and Energy Dispersive X-ray (EDX) studies confirmed the spherical nature of the synthesised particles, as observed by TEM. Fluorescence quenching data of BSA by AgNPs protein corona showed the formation of a 1:1 ground state complex using the Stern–Volmer method. Evaluation of binding parameters and binding energy indicated that the binding reaction was exothermic. In the study of cell cytotoxicity, BSA-AgNPs exhibited greater cytotoxicity than unmodified AgNPs due to the formation of a protein corona, enhancing their suitability for biological applications.

***Index Terms*—Ag Nanoparticles, chemical method, protein interaction, Bovine serum Albumin, Protein corona**

I. INTRODUCTION

Nanotechnology is considered one of the most promising technologies of the twenty-first century, and researchers are exploring its potential as an innovative approach to medical research. Over the past decade, the increase in public funding for nanotechnology research and development suggests that this technology has ushered in a new era of productivity and prosperity [1]. In recent years, inorganic nanoparticles have been utilized in various fields such as medicine, engineering, industry, and food [2][3]. Silver nanoparticles (AgNPs) are widely utilized in products such as refrigerators, mobile phones, clothing, toothbrushes, cosmetics, and medical systems due to their antimicrobial properties [4]. Silver, as an effective antimicrobial agent, has gained popularity for various medical devices. For example, it is proposed to apply silver coatings to implants to prevent the growth of adhering microorganisms and reduce the risk of biofilm-related infections [5,6].

The widespread use of silver nanoparticles (AgNPs) in various fields leads to significant interactions with humans [7–13]. These interactions can occur through

oral medications, wound creams, food packaging, and other means, making it crucial to study how AgNPs interact with human blood. The introduction of AgNPs into the bloodstream and their interactions with plasma proteins are critical for the biomedical applications of these nanoparticles [7,14]. This raises important biosafety concerns regarding nanomaterials. Albumins, the most abundant proteins in plasma, play essential roles in various physiological functions, including transport, buffering, and nutrition. Therefore, any conformational changes in these proteins can significantly impact their functions [3,15–17]. This study uses bovine serum albumin (BSA) because it is structurally similar to human serum albumin, thanks to its unique structural arrangements. BSA is often preferred for research due to its cost-effectiveness and suitability for industrial applications.

When nanoparticles enter a biological medium, they become coated with biomolecules, forming a 'corona' on their surface [18]. this corona alters the physicochemical properties of the nanoparticles and imparts specific biological characteristics [19–21]. The bio-nano interface is established through interactions between the biological entities, the surrounding medium, and the nanoparticle surface [19,22]. These interactions involve classical forces such as electrostatic forces, van der Waals forces, covalent bonds, hydrophobic interactions, and steric effects [14,19]. Recently, there has been a need for a particular focus on the protein corona because of its importance in various therapeutic applications within the biomedical field [23].

Several studies have investigated how surface properties influence the adsorption of proteins and interactions at biological interfaces. However, most of these studies have primarily focused on using proteins as coating materials to enhance the biological acceptance of stable nanomaterials [3,14,24,25]. Recently, Lacerda et al. reported significant interactions between gold nanoparticles and various blood proteins, including albumin, fibrinogen, γ-globulin, histone, and insulin [15]. Their findings suggest that the size of the nanoparticles affects both the binding constants and the adsorption of proteins on their surfaces. Additionally, nanoparticle size significantly influences the conformation of the proteins [15–17].

This work investigates the formation of a protein corona and the structural deformation of bovine serum albumin (BSA) caused by its assembly on the surface of silver nanoparticles (AgNPs). Various spectroscopic techniques and electron microscopy methods were employed, including fluorescence spectroscopy, dynamic light scattering (DLS), Fourier transform infrared (FTIR) spectroscopy, zeta potential measurements, and transmission electron microscopy (TEM) analysis. The interaction between the BSA corona and the surface of the metallic AgNPs was demonstrated through observed changes in the properties of the nanoparticles, as indicated by zeta potential and DLS measurements. This formation of the nanoparticle-protein corona has significant biomedical implications, including antibacterial properties, cell toxicity, drug delivery, and biocompatibility.

II. MATERIALS AND METHODS

2.1. MATERIAL

The following materials were used during the study: Sodium borohydride (crystals) (98%, extra pure, SRL), Silver nitrate (99.5% PCL), D-(+)-glucose (99.5%, Sigma-Aldrich), Sodium hydroxide pellets (98%, Fischer Scientific), and Bovine Serum Albumin (BSA) (98%, SRL).

2.2. EXPERIMENT

2.2.1 SYNTHESIS OF SILVER NANOPARTICLES AND AGNPS PROTEIN CORONA PREPARATION

The 0.01 M solutions of silver nitrate (150 ml) and sodium borohydride (50 ml) were prepared separately. The $AgNO_3$ solution was stirred at 50-60 ℃ for 30 minutes, then the dropwise addition of NaBH4 led to precipitation. The reaction mixture was then kept for 8 hrs. incubation at room temperature. This change in colour occurring during the synthesis was also examined with UV-visible spectra at 200-800 nm. Lastly, AgNPs were collected by centrifugation and dried at 72-80^{0}C ° [26].

The adsorption mechanism of the protein on the nanomaterials plays a crucial role in the protein-nanoparticle corona formation. In this context, the Protein BSA was chosen for corona formation due to its exclusive properties, like its stable nature. The suspensions of the BSA (10 µM) and AgNPs were prepared in Na-phosphate buffer (pH 7.4, 10 mM).

Varied concentrations of the AgNPs (0.05, 0.07, 0.1, 1.0, 1.5, 2.0, and 2.5 µM) were then incubated with a 10 µM BSA solution with a 1:1 stoichiometric ratio, for 1 hour in a shaking incubator [6].

2.3. CHARACTERIZATION

The characterization of AgNPs was carried out between 300 and 500 nm using UV spectroscopy. A JEOL model TEM and JEM 2100 PLUS were used to examine shape, size, and surface features. SEM analysis of AgNPs shows element mapping and shape. X-ray diffraction analysis of AgNPs was conducted using a Bruker AXS D8 Advance instrument, and Fourier transform infrared spectroscopy (FT-IR) was utilised to examine the synthesized nanoparticles triggered by the functional groups present in AgNPs and BSA-AgNPs. Spectrophotometric analysis of the nanoparticles was conducted at room temperature using a Bruker ALPHA FT-IR Spectrophotometer, with spectra reported using a KBr pellet and 4000 to 400 cm^{-1} range. Lastly, laser light scattering with a Malvern Nano ZS90 Instrument was employed to determine the particle size and zeta potential.

III. RESULTS AND DISCUSSION

3.1 CHARACTERISATION OF SILVER NANOPARTICLES

3.1.1. UV-VISIBLE ABSORPTION STUDIES AND XRD ANALYSIS OF SILVER NANOPARTICLES

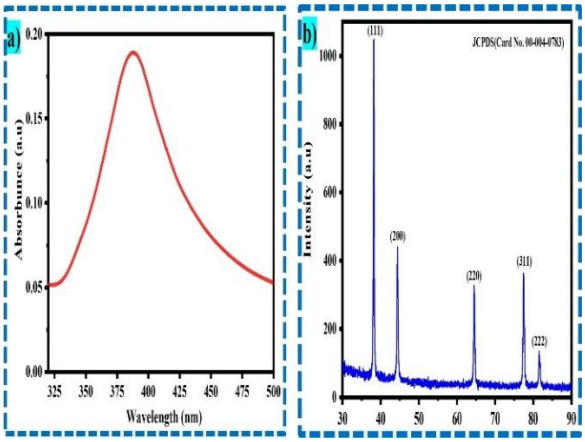

FIG. 1. *A) UV-VISIBLE SPECTRA, B) XRD OF AGNPS*

UV-Vis spectrophotometric analysis was conducted to examine the synthesis of silver nanoparticles (AgNPs). A significant colour change was observed, with the solution transitioning from colourless to a yellowish-brown hue, confirming the synthesis of AgNPs [27]. The absorption spectrum was analysed over a wavelength range of λmax (ε)=200 to 500 nm, indicating the successful synthesis of AgNPs. The effective synthesis of AgNPs was confirmed by a single, broad, and strong surface plasmon resonance (SPR) peak near λmax (ε)= 400 nm in the spectrum, as illustrated in Fig. 1 (a)[28].

To verify the structural characteristics of the AgNPs, X-ray diffraction (XRD) was performed, with the results displayed in Fig. 1(b). The XRD analysis covered a 2θ degree range of 30 to 90 for the AgNPs. The broad peaks in the XRD at 38.13^0, 44.31^0, 64.40^0, $77.51^{0,}$ and 81.48^0 2θ degrees resemble the (111), (200), (220), (311), and (222) (hkl) planes. The observed patterns are compared with JCPDS data (Card No. 00-004-0783), indicating the nanocrystalline structure of AgNPs. The lattice constant parameters a= 4.0862, b= 4.0862, and c=4.0862 confirmed AgNPs' Cubic Crystalline Structure [29].

3.1.2. SEM ANALYSIS OF SILVER NANOPARTICLES

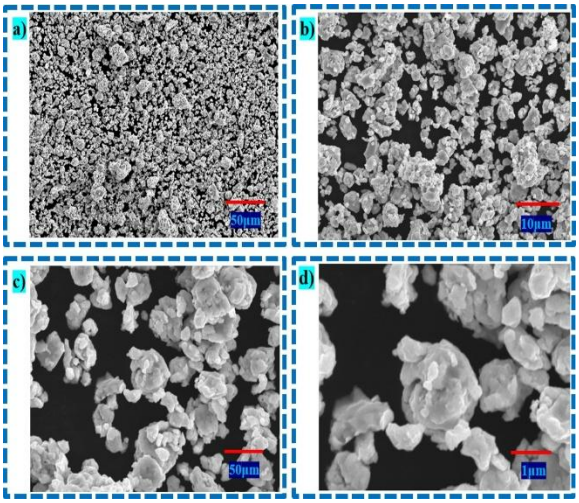

FIG. 2. *SCANNING ELECTRON MICROSCOPY (SEM) ANALYSIS OF* AGNPS

The morphology of the synthesised AgNPs was examined using SEM. The prepared AgNPs exhibited various shapes, including cauliflower-like forms and irregular ellipsoidal shapes as shown in Fig. 2. Furthermore, analysis of the elemental composition through EDX spectral measurements (Fig. S2) reveals

significant peaks for silver, along with additional peaks for carbon and oxygen.

3.2. INTERACTION OF SILVER NANOPARTICLES WITH BOVINE SERUM ALBUMIN (BSA) AND THEIR CHARACTERIZATION

3.2.1 FOURIER-TRANSFORMED INFRARED SPECTROSCOPY (FTIR) SPECTRA OF AGNPS

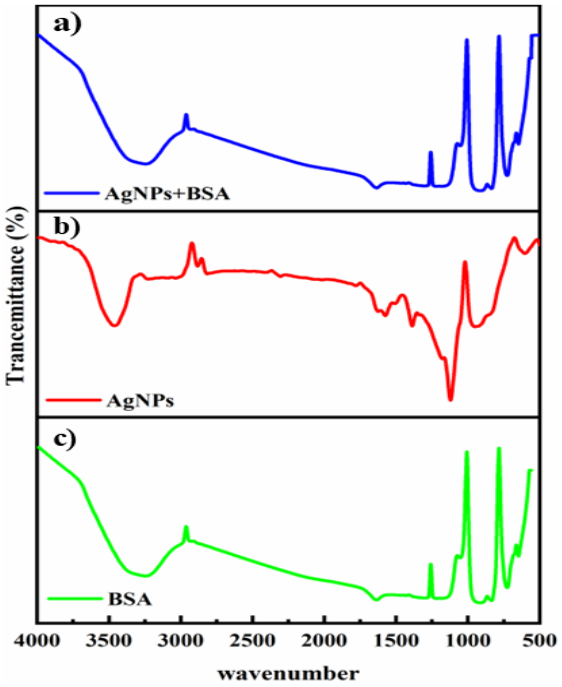

FIG. 3. *FT-IR OF A) AG, B) AG +BSA, C) BSA+AGNPS*

The Fourier-transformed infrared spectroscopy (FTIR) technique is used to observe a material's infrared spectrum. It uses vibrational energy from chemical bonds to extract protein information from NP surfaces. To determine the functional group, the intensity of the observed band is compared to standard values. The absorption band of the material is analyzed to obtain more information. In the FTIR spectra, AgNPs are represented by various peaks. The band at $\tilde{v}$=3462 cm^{-1} in the spectrum represents (-OH) stretching vibration [29][30], [31]. Bands from (C-H) stretching aromatic compounds were seen at $\tilde{v}$=2816 and 2882 cm^{-1}. The (C=C) stretching was given to the band at $\tilde{v}$=1624 cm^{-1}. The (CH_3) deformation group was compared at 1386 cm^{-1} (Fig.S.1). The spectra of the bands at $\tilde{v}$= 1120 cm^{-1}, 954 cm^{-1}, and 482 cm^{-1} are compared to those of the (C-N) group, the CH_2 group[32], and the halogen group, as illustrated by Fig. 3. (a). The FT-IR spectra of BSA+ AgNPs show the disappearance of the absorbance peak of AgNPs, and strong absorbance peaks of BSA were observed, suggesting that BSA forms a strong interaction with AgNPs.

3.2.2. PARTICLE SIZE ANALYSIS AND ZETA POTENTIAL OF AGNPS AND BSA-AGNPS

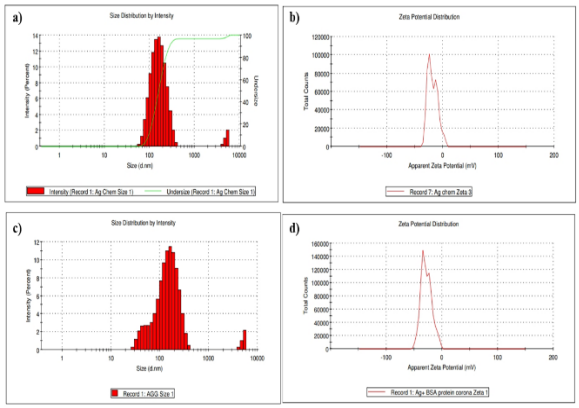

FIG 4. *A) DLS OF AGNPS, B) ZETA-POTENTIAL OF AGNPS, C) DLS OF BSA-AGNPS, D) ZETA-POTENTIAL OF BSA-AGNPS*

Using DLS, the AgNPs distribution of size and zeta potential was identified. Fig. 4 a), b), c), and d) show the results. [33]. According to the DLS results, the size distribution of the silver nanoparticles (AgNPs) showed a Z-average of approximately 113 nm, with a polydispersity index (PDI) of 0.327, indicating a stable suspension (Fig. 4 a, b). However, after interacting with Bovine Serum Albumin (BSA), the size distribution of the AgNPs shifted to 123.3 nm. The Z-average increased, and the PDI rose to 0.822 (Fig. 4 c, d). Additionally, the DLS analysis demonstrated that the thickness of the protein corona around the AgNPs was 10.3 nm, confirming the formation of the protein corona. The zeta potential of AgNPs was measured at -18.1 mV, and after interacting with BSA, the zeta potential changed to -30.4 mV[33]. This significant change in mV indicates the formation of a protein corona around the AgNPs, suggesting increased stability [26,30].

3.2.3. TEM ANALYSIS OF AGNPS AND BSA-AGNPS: A COMPARISON OF PARTICLE SIZES

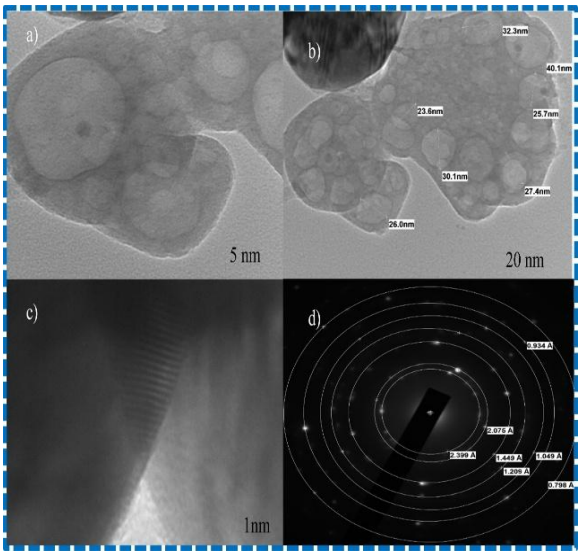

FIG. 5. *A) AND B) TEM IMAGES OF AGNPS, C) AN ENLARGED VIEW OF A SINGLE PARTICLE SHOWING A LATTICE FRINGE OF 0.526NM, AND D) ELECTRON DIFFRACTION.*

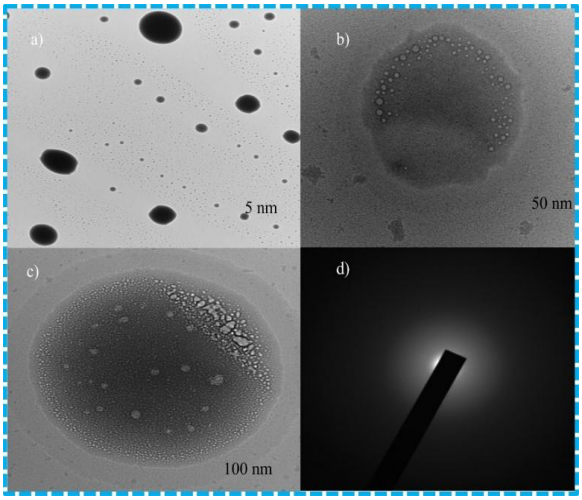

FIG. 6. *A) AND B) TEM IMAGES OF BSA-AGNPS, C) AN ENLARGED VIEW OF A SINGLE PARTICLE OF BSA-AGNPS, D) ELECTRON DIFFRACTION PATTERN OF BSA-AGNPS.*

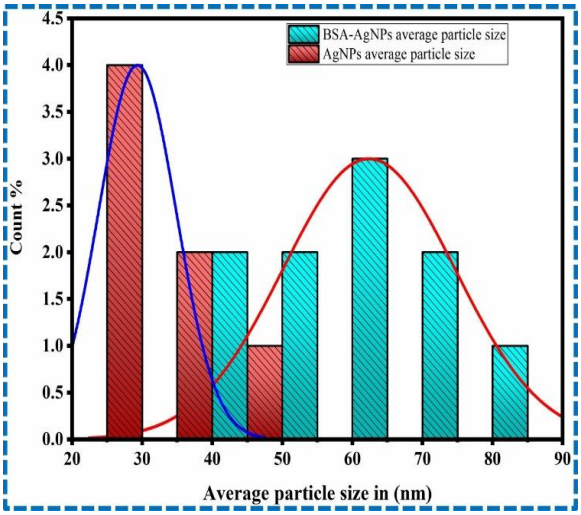

FIG. 7. *PARTICLE SIZE COMPARISON OF AGNPS AND BSA-AGNPS,*

The Transmission Electron Microscopy (TEM) analysis was performed to get a better view of AgNPs and the protein corona of AgNPs. Fig. 5a represents a TEM micrograph of the AgNPs, which shows a uniform distribution of spherical-shaped particles. The average particle size was 29.31 nm (Fig.7). According to current literature, AgNPs ranging from 10 to 30 nm can easily penetrate cell membranes, potentially destroying harmful cell lines. Additionally, smaller nanoparticles tend to have a higher affinity for forming a protein corona [34]. The Selected Area Electron Diffraction (SAED) pattern, displayed in Fig. 5d, reveals bright rings and a spotty pattern. This indicates the presence of various lattice planes, confirming the nanocrystalline nature of the AgNPs. Further, the AgNPs and their protein corona were analysed by TEM. Fig. (6 b, c) displays the TEM images of the protein corona formed by bovine serum albumin (BSA) around the synthesised AgNPs. (Fig. 6.a) shows that the corona surrounding the AgNPs is uniform; however, the size of the corona varies from one particle to another. The average particle size of BSA-AgNPs was 60.75 nm (Fig.7). The selected area electron diffraction (SAED) graph of the BSA-AgNPs plane disappeared, as the binding of the protein with the nanoparticle complicates its representation.

3.2.4 FLUORESCENCE QUENCHING OF BSA ON INTERACTION WITH SYNTHESISED AGNPS

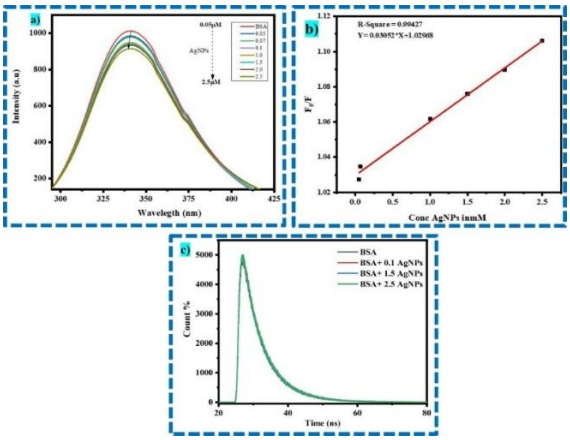

FIG. 8. A) *FLUORESCENCE SPECTRA OF BSA WITH INCREASING CONCENTRATIONS OF AGNPS, B) STERN VOLMER PLOT OF BSA-AGNPS, C) FLUORESCENCE LIFETIME OF BSA-AGNPS*

Fluorescence quenching is a popular approach for measuring alterations in protein structure and influencing the local structural dynamics and environment of tryptophan in BSA [35]. Here, the adsorption process of proteins and AgNPs has been examined and analysed using the fluorescence spectroscopic method. The advantage of using a fluorescence probe is that binding constants can be found without separating bound or unbound proteins[16].

Fig. 8 displays the fluorescence emission spectra of BSA and BSA treated with AgNPs at 295 nm. The fluorescence intensity of BSA decreases gradually with increasing concentration of AgNPs from 0.05μM to 2.5μM with a slight blue shift observed. [12]. This decreasing fluorescence intensity and blue shift suggested that AgNPs influence the tryptophan microenvironment in BSA. The fluorescence quenching can be caused by several reasons, mainly described by static and dynamic quenching mechanisms. In dynamic quenching, the interaction of fluorophore and quencher happens on an excited state, while in the case of static quenching, ground-state complex formation was responsible for energy discharge. Generally, a non-fluorescent ground state complex was formed in static quenching between the fluorophore and quencher. When a complex absorbs light, it immediately returns to the ground state without the emission of a photon [36,37]. The linear plot of F_0/F V/s concentration of AgNPs (μM) follows the Stern-Volmer equation (1)

$$\frac{F0}{F} = 1 + Ksv[Q] \quad \ldots\ldots\ldots (1)$$

where F_0 and F are the fluorescence intensity of BSA before and after the addition of AgNPs, while Ksv is the Stern-Volmer constant and [Q] concentration of AgNPs (μM). The linear relation cannot prove the static or dynamic quenching mechanism Fig. 8 b). The key difference between static and dynamic quenching is the change. In fluorescence lifetime in the case of static quenching, a ratio of fluorescence lifetime (τ) equals 1, while for dynamic quenching, $F_0/F = \tau_0/\tau$. Herein, the fluorescence lifetime of BSA with AgNPs was measured as shown in Fig. 8. c. No change was observed in the fluorescence lifetime of BSA and various concentrations of AgNPs with BSA. Hence, the value of $\tau_0/\tau = 1$, where τ is the fluorescence lifetime. The data suggested that the interaction between BSA and AgNPs was due to ground-state complex formation, which confirmed the formation of a protein CORONA.

3.3 CYTOTOXIC ACTIVITY

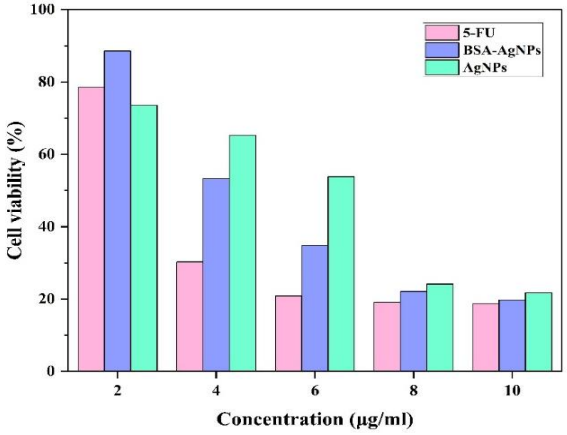

FIG. 9. *CYTOTOXICITY OF AGNPS AND BSA-AGNPS AGAINST BREAST CANCER (MCF-7) CELL LINE*

Silver nanoparticles (AgNPs) have received significant attention in nanomedicine due to their potent anticancer properties. However, their interaction with biomolecules in biological systems often leads to the formation of a protein corona, a layer

of proteins that adsorb onto the nanoparticle surface. This corona alters the physicochemical properties of the nanoparticles, influencing their biological interactions and therapeutic potential.

A comparative cytotoxicity study of unmodified AgNPs and BSA-AgNPs on the MCF-7 breast cancer cell line demonstrated notable differences in their efficacy (Fig. 9). After 24 hours of treatment, the AgNPs-protein corona exhibited higher cytotoxicity, significantly reducing MCF-7 cell viability at an IC_{50} value of 3.37 ± 0.67 µg/ml. This effect was markedly greater than that observed for unmodified AgNPs, which had an IC_{50} value of 6.39 ± 0.48 µg/ml. For comparison, 5-Fluorouracil, a standard chemotherapeutic agent, showed an IC_{50} value of 2.67 ± 0.03 µl/ml (Fig. 9). These results suggest that the formation of a protein corona enhances the cytotoxic potential of AgNPs, potentially due to improved cellular uptake or altered interaction mechanisms with cancer cells. This study underscores the importance of understanding nanoparticle-protein interactions for optimizing nanomedicine applications in cancer therapy [38] (Fig. 9).

The present study supports the current literature that AgNPs-protein corona induced cytotoxicity in a dose-dependent manner [38]. This is consistent with previous findings, which suggest that BSA enhances the dissolution kinetics of AgNPs in cancer cells as a function of their size and concentration. A large amount of BSA adheres to Ag+ and accelerates its dissolution. When AgNPs are coated with BSA, the dissolution of AgNPs is enhanced. AgNP dissolution is slowed down further once the BSA molecules have fully coated the surface and created silver-sulfide linkages [21]. According to one study[39]The degree to which BSA is present on the AgNPs surface increases the oxidative release of Ag ions, and the size of the particles influences these enhancements.

IV. CONCLUSION

Understanding the formation of the protein-nanoparticle corona is crucial for advancing the design of nanomaterials and expanding their potential applications in biomedicine. This study explored the characteristics of bovine serum albumin-coated silver nanoparticles (BSA-AgNPs), focusing on their surface charge, morphology, and size. Results from dynamic light scattering (DLS) and transmission electron microscopy (TEM) confirmed that the presence of the BSA protein corona increases the particle size compared to bare AgNPs. Zeta potential measurements indicated changes in surface charge after protein adsorption, suggesting that the BSA-coated nanoparticles have enhanced stability. Fourier-transform infrared (FT-IR) spectroscopy verified the presence of protein functional groups on the nanoparticle surface, supporting the successful formation of the corona.

Additionally, Stern-Volmer analysis demonstrated static quenching behavior, indicating a dose-dependent interaction between BSA and AgNPs. Importantly, BSA-AgNPs exhibited greater cytotoxicity than uncoated AgNPs, highlighting their potential for targeted biological and therapeutic applications.

ACKNOWLEDGMENT

Thanks to BARTI for providing financial support through research fellowships under the BANRF 2020 scheme and to the Common Facility Centre (CFC) at the Sophisticated Instrumentation Facility Centre (SAIF), Kolhapur, for characterizing the research instruments.

REFERENCES

[1] A. Haleem, M. Javaid, R.P. Singh, S. Rab, R. Suman, Applications of nanotechnology in medical field: a brief review, Glob. Heal. J. 7 (2023) 70–77. https://doi.org/10.1016/j.glohj.2023.02.008.

[2] X. Zhang, Z. Liu, W. Shen, S. Gurunathan, Silver Nanoparticles: Synthesis, Characterization, Properties, Applications, and Therapeutic Approaches, (2016). https://doi.org/10.3390/ijms17091534.

[3] N. Dasgupta, S. Ranjan, D. Patra, P. Srivastava, A. Kumar, C. Ramalingam, Chemico-Biological Interactions Bovine serum albumin interacts with silver nanoparticles with a “side- on” or “end on” conformation, 253 (2016) 100–102.

[4] P.M. Seumo Tchekwagep, J.H. Eminovski, C.P. Nanseu-Njiki, E. Ngameni, T. Arnebrant, T. Ruzgas, Adsorption of Bovine Serum Albumin on Silver Nanoparticle Layer Deposited on Mercaptohexylpyridinium-Coated Quartz Crystal Microbalance with Dissipation Gold Electrode:

Studied by Electrochemical Quartz Crystal Microbalance with Dissipation, Phys. Status Solidi Appl. Mater. Sci. 217 (2020) 1–7. https://doi.org/10.1002/pssa.201900839.

[5] M.A. Wassall, M. Santin, C. Isalberti, M. Cannas, S.P. Denyer, Adhesion of bacteria to stainless steel and silver-coated orthopedic external fixation pins, J. Biomed. Mater. Res. 36 (1997) 325–330. https://doi.org/10.1002/(SICI)1097-4636(19970905)36:3<325: AID-JBM7>3.0.CO;2-G.

[6] N. Dasgupta, S. Ranjan, D. Patra, P. Srivastava, A. Kumar, C. Ramalingam, AC SC, Chem. Biol. Interact. (2016). https://doi.org/10.1016/j.cbi.2016.05.018.

[7] S. Das, L. Langbang, M. Haque, V.K. Belwal, K. Aguan, A. Singha Roy, Biocompatible silver nanoparticles: An investigation into their protein binding efficacies, anti-bacterial effects and cell cytotoxicity studies, J. Pharm. Anal. 11 (2021) 422–434. https://doi.org/10.1016/j.jpha.2020.12.003.

[8] C. Vanlalveni, S. Lallianrawna, A. Biswas, M. Selvaraj, B. Changmai, S.L. Rokhum, Green synthesis of silver nanoparticles using plant extracts and their antimicrobial activities: a review of recent literature, RSC Adv. 11 (2021) 2804–2837. https://doi.org/10.1039/d0ra09941d.

[9] N.P.U. Nguyen, N.T. Dang, L. Doan, T.T.H. Nguyen, Synthesis of Silver Nanoparticles: From Conventional to 'Modern' Methods—A Review, Processes. 11 (2023). https://doi.org/10.3390/pr11092617.

[10] N. Durán, C.P. Silveira, M. Durán, D.S.T. Martinez, Silver nanoparticle protein corona and toxicity: a mini - review, J. Nanobiotechnology. (2015) 1–17. https://doi.org/10.1186/s12951-015-0114-4.

[11] S. V Banne, M.S. Patil, R.M. Kulkarni, S.J. Patil, ScienceDirect Synthesis and Characterization of Silver Nano Particles for EDM Applications, Mater. Today Proc. 4 (2017) 12054–12060. https://doi.org/10.1016/j.matpr.2017.09.130.

[12] A. Almatroudi, Silver nanoparticles: Synthesis, characterisation and biomedical applications, Open Life Sci. 15 (2020) 819–839. https://doi.org/10.1515/biol-2020-0094.

[13] K.M. Mahmud, M.M. Hossain, S.A. Polash, M. Takikawa, M.S. Shakil, M.F. Uddin, M. Alam, M.M. Ali Khan Shawan, T. Saha, S. Takeoka, M.A. Hasan, S.R. Sarker, Investigation of Antimicrobial Activity and Biocompatibility of Biogenic Silver Nanoparticles Synthesized using Syzigyum cymosum Extract, ACS Omega. 7 (2022) 27216–27229. https://doi.org/10.1021/acsomega.2c01922.

[14] S.M. Ahsan, C.M. Rao, Nanoparticle-Protein Interaction: The Significance and Role of Protein Corona, (2018).

[15] A. Manuscript, rsc.li/njc, (2017). https://doi.org/10.1039/C7NJ01227F.

[16] G.R. Smith, M.J.E. Sternberg, P.A. Bates, the relationship between the flexibility of proteins and their conformational states on forming protein-protein complexes with an application to protein-protein docking, J. Mol. Biol. 347 (2005) 1077–1101. https://doi.org/10.1016/j.jmb.2005.01.058.

[17] C. Guo, X. Guo, W. Chu, N. Jiang, H. Li, Spectroscopic study of conformation changes of bovine serum albumin in aqueous environment, Chinese Chem. Lett. 30 (2019) 1302–1306. https://doi.org/10.1016/j.cclet.2019.02.023.

[18] W. Huang, G. Xiao, Y. Zhang, W. Min, Research progress and application opportunities of nanoparticle–protein corona complexes, Biomed. Pharmacother. 139 (2021) 111541. https://doi.org/10.1016/j.biopha.2021.111541.

[19] L. Abarca-Cabrera, P. Fraga-García, S. Berensmeier, Bio-nano interactions: binding proteins, polysaccharides, lipids and nucleic acids onto magnetic nanoparticles, Biomater. Res. 25 (2021) 1–18. https://doi.org/10.1186/s40824-021-00212-y.

[20] N. Nerlekar, P. Patil, S. Khot, A. Kulkarni, P. Dandge, A. Berde, S. Kamane, P. Ghatage, P. Dandge, Cold maceration extraction of wild fruit Terminalia bellirica (Gaertn.) Roxb.: exploring its bioactives for biomedical applications, Prep. Biochem. Biotechnol. 0 (2024) 1–19. https://doi.org/10.1080/10826068.2024.2313632.

[21] P. Patil, N. Nerlekar, S. Rathod, P. Mhaldar, T. Najm, P. Bansode, J. Jadhav, P. Dandge, P. Choudhari, D. Pore, G. Rashinkar, Novel sulphonamide-azaheterocycle conjugates and their anti-cancer, anti-inflammatory, anti-diabetic, anti-angiogenesis activity and molecular docking studies, Results Chem. 7 (2024) 101476. https://doi.org/10.1016/j.rechem.2024.101476.

[22] N.P. Corona, Y. Li, J. Lee, Insights into Characterization Methods and Biomedical Applications of, (2020).

[23] V. Gorshkov, J.A. Bubis, E.M. Solovyeva, M. V. Gorshkov, F. Kjeldsen, Protein corona formed on silver nanoparticles in blood plasma is highly selective and resistant to physicochemical changes of the solution, Environ. Sci. Nano. 6 (2019) 1089–1098. https://doi.org/10.1039/c8en01054d.

[24] R. Abbasi, G. Shineh, M. Mobaraki, S. Doughty, L. Tayebi, Structural parameters of nanoparticles affecting their toxicity for biomedical applications: a review, Springer Netherlands, 2023. https://doi.org/10.1007/s11051-023-05690-w.

[25] T. Kopac, International Journal of Biological Macromolecules Protein corona, understanding the nanoparticle – protein interactions and future perspectives: A critical review, Int. J. Biol. Macromol. 169 (2021). https://doi.org/10.1016/j.ijbiomac.2020.12.108.

[26] Y.Z. Zhao, D.X. Du, Y.H. Wang, Preparation of silver nanoparticles and application in water-based conductive inks, Int. J. Mod. Phys. B. 33 (2019) 1–14. https://doi.org/10.1142/S0217979219503855.

[27] A.K. Giri, B. Jena, B. Biswal, A.K. Pradhan, M. Arakha, S. Acharya, L. Acharya, Green synthesis and characterization of silver nanoparticles using Eugenia roxburghii DC. extract and activity against biofilm-producing bacteria, Sci. Rep. 12 (2022) 1–9. https://doi.org/10.1038/s41598-022-12484-y.

[28] J. Chauhan, V.R. Mehto, T. Tiwari, Chemical Synthesis and Study of Silver Nanoparticles, (2019).

[29] K. Jyoti, M. Baunthiyal, A. Singh, Characterization of silver nanoparticles synthesized using Urtica dioica Linn. leaves and their synergistic effects with antibiotics, J. Radiat. Res. Appl. Sci. 9 (2016) 217–227. https://doi.org/10.1016/j.jrras.2015.10.002.

[30] M.H. Ali, M.A.K. Azad, K.A. Khan, M.O. Rahman, U. Chakma, A. Kumer, Analysis of Crystallographic Structures and Properties of Silver Nanoparticles Synthesized Using PKL Extract and Nanoscale Characterization Techniques, ACS Omega. 8 (2023) 28133–28142. https://doi.org/10.1021/acsomega.3c01261.

[31] I. Jahan, F. Erci, I. Isildak, Rapid green synthesis of non-cytotoxic silver nanoparticles using aqueous extracts of “Golden Delicious” apple pulp and cumin seeds with antibacterial and antioxidant activity, SN Appl. Sci. 3 (2021) 1–14. https://doi.org/10.1007/s42452-020-04046-6.

[32] S. Faisal, M.H. Tariq, Abdullah, S. Zafar, Z. Un Nisa, R. Ullah, A. Ur Rahman, A. Bari, K. Ullah, R.U. Khan, Bio synthesis, comprehensive characterization, and multifaceted therapeutic applications of BSA-Resveratrol coated platinum nanoparticles, Sci. Rep. 14 (2024) 1–21. https://doi.org/10.1038/s41598-024-57787-4.

[33] H. Yang, C. Hao, Z. Nan, R. Sun, Bovine hemoglobin adsorption onto modified silica nanoparticles: multi-spectroscopic measurements based on kinetics and protein conformation, Int. J. Biol. Macromol. 155 (2020) 208–215. https://doi.org/10.1016/j.ijbiomac.2020.03.211.

[34] S. Tang, J. Zheng, Antibacterial Activity of Silver Nanoparticles: Structural Effects, 1701503 (2018) 1–10. https://doi.org/10.1002/adhm.201701503.

[35] C.J. Fossum, B.O.V. Johnson, S.T. Golde, A.J. Kielman, B. Finke, M.A. Smith, H.R. Lowater, B.F. Laatsch, S. Bhattacharyya, S. Hati, Insights into the Mechanism of Tryptophan Fluorescence Quenching due to Synthetic Crowding Agents: A Combined Experimental and Computational Study, ACS Omega. 8 (2023) 44820–44830. https://doi.org/10.1021/acsomega.3c06006.

[36] M. Mahanthappa, M.A. Savanur, J. Ramu, A. Tatagar, Elucidating the significance of molecular interaction between sulphur doped zinc oxide nanoparticles and serum albumin using multi spectroscopic approach, J. Mol. Recognit. 36 (2023) 1–14. https://doi.org/10.1002/jmr.3054.

[37] N. Hlapisi, P.A. Ajibade, Preparation of pure phase silver nanoparticles: Morphological, optical, binding interactions with bovine serum albumin and antioxidant potential studies, J. Mol. Struct. 1322 (2025) 140219. https://doi.org/10.1016/j.molstruc.2024.140219.

[38] N.A. Razak, N. Abu, W.Y. Ho, N.R. Zamberi, S.W. Tan, N.B. Alitheen, K. Long, S.K. Yeap, Cytotoxicity of eupatorin in MCF-7 and MDA-MB-231 human breast cancer cells via cell cycle arrest, anti-angiogenesis and induction of apoptosis, Sci. Rep. 9 (2019) 1–12. https://doi.org/10.1038/s41598-018-37796-w.

[39] M. Lundqvist, J. Stigler, G. Elia, I. Lynch, T. Cedervall, K.A. Dawson, Nanoparticle size and surface properties determine the protein corona with possible implications for biological impacts, Proc. Natl. Acad. Sci. U. S. A. 105 (2008) 14265–14270. https://doi.org/10.1073/pnas.0805135105